SEMARAK ILMU PUBLISHING

Journal of Advanced Research in Fluid Mechanics and Thermal Sciences

Journal homepage:
https://semarakilmu.com.my/journals/index.php/fluid_mechanics_thermal_sciences/index
ISSN: 2289-7879

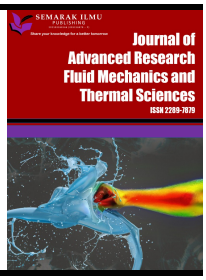

Numerical Study on Heat Transfer Characteristics of Jet Impingement by using MgO Nanofluid

Tan Zhi Xian[1], Tang Tsz Loong[1], Hamidon Salleh[1,*], Hasan Abdualatif Muhalhal[3], Nur Syahirah Mohd Hanafi[2], Intan Fadhlina Mohamed[2], Mohd Anas Mohd Sabri[2], Wan Aizon Wan Ghopa[2]

[1] Department of Energy and Thermofluid Engineering, Faculty of Mechanical and Manufacturing Engineering, Universiti Tun Hussein Onn, Parit Raja, 86400 Batu Pahat, Johor, Malaysia
[2] Department of Mechanical and Manufacturing Engineering, Faculty of Engineering & Built Environment, Universiti Kebangsaan Malaysia, 43600 Bangi, Selangor, Malaysia
[3] Department of Marine Mechanical Engineering, Al Asmarya Islamic University, Zliten, Libya

ARTICLE INFO

Article history:
Received 12 July 2024
Received in revised form 23 Sept. 2024
Accepted 1 October 2024
Available online 20 October 2024

Keywords:
ANSYS workbench 18.2; ANSYS fluent; heat transfer characteristics; multiple jet impingement; magnesium oxied nanofluid; numerical simulation; Reynolds number; volume concentration

ABSTRACT

Liquid impingement jet can provide high local heat transfer coefficients between the impinged liquid and the targeted surface. Jet impingement is utilized in the applications which is related to rapid cooling and better control of high temperature in many applications. The studies are carried out numerically by using ANSYS Workbench 18.2. Hexagonal meshing and Shear-Stress Transport (SST) turbulence model is used in the numerical simulation. By using SST turbulence model, the effect of jet Reynolds number, nanofluid volume concentration on the average heat transfer coefficient of the target plate is analysed and discussed. For the effect of varying the Reynolds number, it is observed that the surface average heat transfer coefficient increases at least 76.18% as the Reynolds number increases from 5000 to 10000. Moreover, the heat transfer coefficient increases as the volume concentration increases from 0% to 5%. It is also observed that when the nanofluid with higher thermal conductivity will results in higher heat transfer coefficient where the MgO nanofluid showed the highest heat transfer coefficient. As a conclusion, by increasing Reynolds number, volume concentration and thermal conductivity of nanofluid, the heat transfer coefficient can be enhanced.

1. Introduction

Liquid impingement jet is a technique that can deliver great local heat transfer between the fluid and the target plate. Jet impingement was utilized in the applications which is associated with better control of high temperature and rapid cooling in many industrial applications [1,2]. Tang *et al.,* [3] conducted a numerical investigation showing the significance of jet impingement systems in achieving high heat flux rates, especially in cooling applications. Recent studies highlight that jet impingement heat transfer is especially beneficial in cooling applications with high localized heat flux requirements, such as electronics and turbine systems [4,5]. Waware, Kore and Patil [6] highlighted

* *Corresponding author.*
E-mail address: hamidon@uthm.edu.my

https://doi.org/10.37934/arfmts.122.2.202218

similar applications of impingement jets in enhancing cooling efficiency in high-temperature processes, demonstrating their versatility in industrial settings. Impinging jet research can be conducted to evaluate and study the heat transfer coefficient. It had been identified that the heat transfer coefficients will vary with the distance from the impact plate [7]. The liquid impingement jet can be classified into two types which are the submerged jet and the free surface jet. Submerged jet is formed when the liquid impingement jet is discharged within the same medium. Whereas, as the liquid jet discharges into less dense medium, the free surface jet is formed. Free surface jet had been reported that it shows higher capacity of cooling [1,8]. The jet generated from nozzle with the temperature and profile and the characteristics of turbulence which is reliant on the upstream flow. The flow pattern in the nozzle develops into parabolic velocity profile. After exit from the nozzle, velocity gradient of the emerging jet which generate the shearing at the jet boundaries which it able to transfer momentum horizontally outward and pulling extra fluid laterally with the jet and increase the mass flow of the jet [9].

In this research, numerical simulation of multiple (3×3) impingement jet on the flat plate had been conducted. This research is aimed to study the phenomenon of varying the Reynolds number and volume concentration of nanofluid on the heat transfer characteristics of jet impingement. This study will use ANSYS Fluent 18.1 as a CFD simulation software to carry out numerical solution. 9 jet nozzles with the angle α of the impinging jet is 90°.are used. The heat transfer fluid used is magnesium oxide nanofluid. The nozzle-to-plate distance used is 3 mm. The nozzle diameter and jet-to-jet distance is 1 mm and 3 mm respectively. While the concentration of nanofluid used is 0%, 1%, 2%, 3%, 4% and 5%. The Reynolds number of the flow is 5000, 6000, 7000, 8000, 9000 and 10000.

The conceptual design should be passed through the design phases as in the format which allows simple application of the suitable analysis method. The accuracy of the numerical simulation result is mostly affected by the quality of mesh or the surface discretization [10]. There are several types of meshing in terms of element shapes such as triangle and quadrilateral mesh of 2D cell types while tetrahedron, hexahedron, prism, pyramid and polyhedron mesh for 3D cell types [11]. For hexahedron mesh, it required lest number of elements to resolve most of the CFD problems and it can be used to predict the near wall flow activity and increase quality of mesh.

Many of the industrial applications are concerned with turbulence flow in the whole domain. Over the years, various turbulence models have been developed to roughly predict the impingement flow and heat transfer. But there are only a limited number of studies concerned with comparisons of reliability, availability and capability of different turbulence models for impingement flow [12]. Faris Abdullah *et al.,* [13] emphasized the importance of choosing the correct turbulence model, particularly for impingement jet flows where mesh quality significantly affects numerical accuracy. SST turbulence model can be considered as one of the most successful models where it combines model which is near the wall and model which is further than from the wall to employ the advantages of each model. The SST model predicts mean velocities better than the models and is among the uncertainty of the experimental results. Additional studies have shown that the SST model, when paired with high-quality mesh, can provide accurate predictions for complex fluid flow scenarios, ensuring reliable heat transfer data [14]. This shows that the SST model can predict good numerical solution but with a lower computational cost [9,12,15,16].

2. Methodology

The numerical domain is occupied with water-MgO nanofluid. The 3-D Navier-Stokes and energy equations with the standard turbulence model are solved by using commercial CFD software (ANSYS Fluent) which are combined with the momentum and the continuity equations to simulate the

turbulence and thermal flow fields. Putranto and Utomo [17] and Nasir *et al.,* [18] emphasized the importance of choosing the correct simulation model to ensure the accuracy of results. The SST turbulence model is used in this research. Ng *et al.,* [19] emphasized that proper turbulence modelling, as implemented in this study using the SST model, is key to achieving accurate heat transfer predictions in impingement jet studies. The flow inside the jet is assumed to be steady, incompressible and three-dimensional flow. The radiation heat transfer effects and the buoyancy are ignored and thermo-physical properties of the fluid are expected to be constant. The radiation heat transfer effects and the buoyancy are ignored and thermo-physical properties of the fluid are expected to be constant. The schematic diagram of the physical geometry and computational domain are shown in Figure 1.

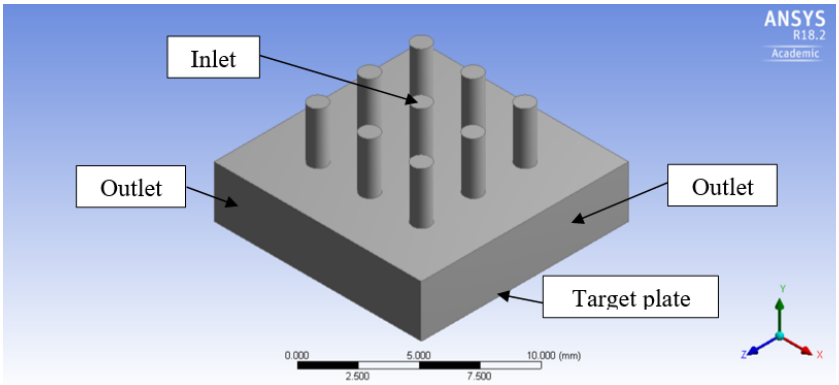

Fig. 1. Schematic diagram of computational domain

2.1 Numerical Domain

The bottom partition of the numerical domain was the bottom surface of the target plate. It is expected that the heat was generated at a uniform rate inside the heat sink base and can be generated by a constant heat flux from the bottom surface of the target plate. If the heat flux from the bottom surface is not dissipated well, the temperature of the target plate will increase and may cause failure of components on which target plate is mounted. Nanofluid flows through 1 mm diameter jet nozzles with high velocity directly to the target plate of 12 mm ×12mm with 3 mm thickness. After impingement, the flow of the jet will exit from the outlet. Figure 2 represents the details of the nozzle plate geometry.

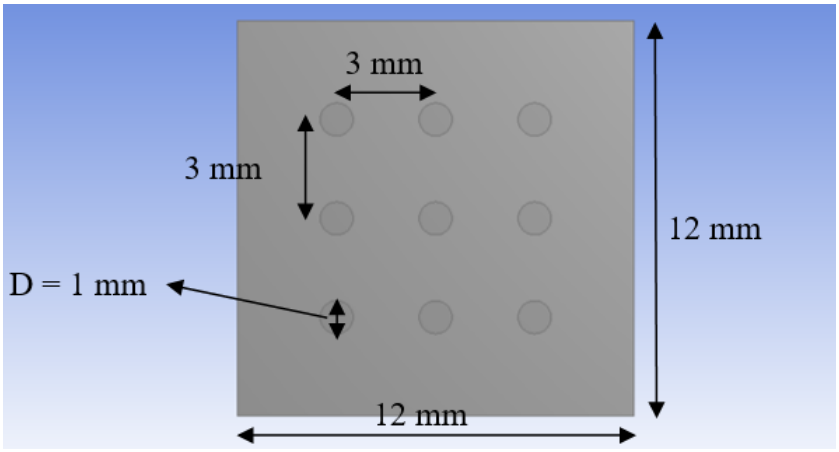

Fig. 2. Geometry of nozzle plate

2.2 Mesh Generation and Grid Independence Test

The computational domain has been divided into several structural meshes. As structural mesh used is the hexagonal mesh, the precise prediction of heat transfer characteristics is possible [15]. Hexagonal mesh is applied throughout the whole numerical domain and to predict the near wall flow phenomenon. Inflation technique is used. Figure 3 represents the mesh domain of the numerical model of multiple jet impingement.

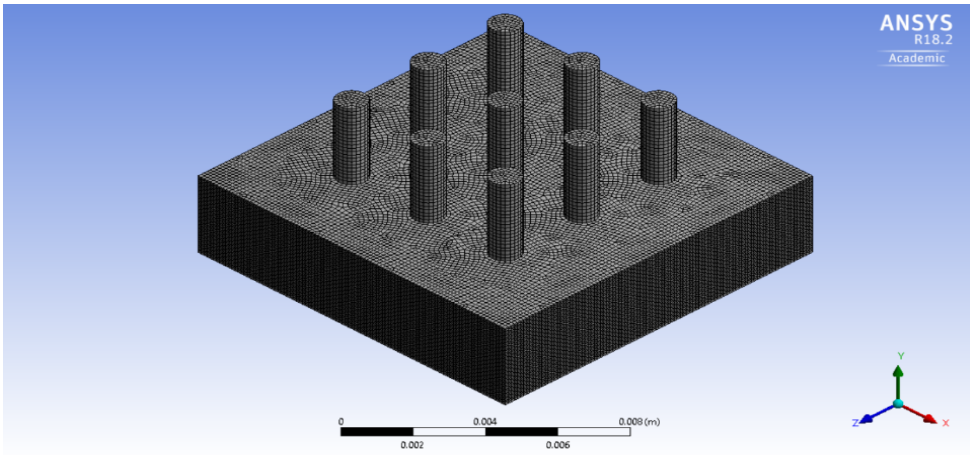

Fig. 3. Mesh domain of the numerical model of the multiple jet impingement

Grid independence test (GIT) or known as mesh independence study is used to establish accurate numerical solution. Grid independence test is conducted by developing three different mesh which are coarse, medium and fine mesh [15,16]. Mesh resolution plays a crucial role when generating final numerical solution, where the grid independence test was carried out to minimize the discretization error [19]. Abdul-Rahman and Mohammad Rasani [20] recommended mesh independence studies as critical in reducing errors during turbulence model simulations, particularly in multi-jet configurations. The grid independence on heat transfer characteristics were checked by increasing the number of elements of the numerical model from 22680 cells and the mesh is independent when the number of elements reach 489154 cells.

2.3 Boundary Conditions

The numerical domain is filled with MgO nanofluid. The 3-D Navier-Stokes and energy equations with SST turbulence model are solved using ANSYS Fluent which combined continuity and momentum equations to simulate thermal and turbulence flow fields. Where shear stress transport (SST) turbulence model was found to work the best among the available turbulence models for impingement jet.

The buoyancy and radiation heat transfer effects are neglected and thermo physical properties of the fluid such as density, specific heat and thermal conductivity are assumed to be constant. In their CFD analysis of multi-jet impingement, Zainodin, Anuar Jamaludin and Pop [21] confirmed that the choice of boundary conditions significantly impacts the accuracy of heat transfer predictions. The boundary conditions of the impingement jet are stated as:

i. Velocity Inlet: At the inlet boundary, Reynolds number of the nanofluid impingement jet are specified. The velocity of flow is calculated based on the specified Reynolds number where the Reynolds number varied from 5000 to 10000. A constant temperature of 300 K is prescribed.
ii. Wall surface: No slip condition and 300 K temperature had been applied.
iii. Pressure Outlet: At the pressure exit boundary, 0 Pa pressure outlet, 300 K constant temperature and turbulence intensity of 5% are specified.
iv. Plate: At the plate domain, no slip condition and constant heat flux of 877066.7 W/m2 are specified.

2.4 Numerical Solver

A geometry of the multiple jet impingement is imported into ANSYS Fluent software to solve the governing equations. The flow and turbulence fields must be solved correctly to get reasonable prediction of heat transfer characteristics and the flow pattern of the jet impingement. Second order upwind scheme is applied on all terms which will affect the heat transfer. The SIMPLE algorithm is used for the pressure-velocity coupling. Steady state condition, 10E-6 residuals for converging criteria and 10000 maximum iterations is applied throughout all the simulation which carried out in this research.

2.5 Thermo-Physical Properties
2.5.1 Density of MgO nanofluid

The thermo-physical properties of MgO nanofluid are identified at the fluids' bulk mean temperature by using the widely used correlation equations in the literature. The density of the nanofluid can be calculated by using density correlation equation as show in Eq. (1) [22].

$$\rho_{nf} = \emptyset\rho_p + (1 - \emptyset)\rho_{bf} \quad (1)$$

Where: ρ_{nf} is the density of MgO nanofluid, $\emptyset$ is the MgO nanofluid concentration, ρ_p is the density of MgO nanoparticles and ρ_{bf} is the density of base fluid (water).

2.5.2 Specific heat of MgO nanofluid

The specific heat is one of the important properties and plays an important role in affecting the rate of heat transfer of MgO nanofluid. Specific heat can be defined as the amount of heat required to raise the temperature of 1 gram of nanofluid by 1℃. For a given volume concentration of MgO nanofluid, the specific heat can be obtained by using mixture formula as shown in Eq. (2).

$$C_{P-nf} = \left[(1 - \emptyset)(\rho C_P)_{bf} + \emptyset(\rho C_P)_P\right] / \left[(1 - \emptyset)\rho_{bf} + \emptyset\rho_P\right] \quad (2)$$

Where: C_{P-nf} is the specific heat of MgO nanofluid, C_{P-bf} is the specific heat of base fluid and C_{P-P} is the specific heat of MgO nanoparticle.

2.5.3 Thermal conductivity of MgO nanofluid

Based on Bruggeman model which is effective for the spherical particles and it also think over the interaction between the nanoparticles, the thermal conductivity of nanofluid can be obtained by using Eq. (3) [22]. Other research also demonstrates that MgO nanofluids exhibit a significant increase in thermal conductivity, enhancing their potential in high-efficiency cooling applications [23].

$$K_{nf} = [1/4]\left[(3\emptyset - 1)K_{MgO} + (2 - 3\emptyset) - K_{bf}\right] + \left[K_{bf}/4\right]\sqrt{\Delta} \quad (3)$$
$$\Delta = \left[(3\emptyset - 1)^2\left(K_{MgO}/K_{bf}\right)^2 + (2 - 3\emptyset)^2 + 2(2 + 9\emptyset - 9\emptyset^2)\left(K_{MgO}/K_{bf}\right)\right]$$

Where: K_{nf} is the thermal conductivity of magnesium oxide nanofluid, K_{MgO} is the thermal conductivity of magnesium oxide particles and K_{bf} is the thermal conductivity of base fluid.

2.5.4 Viscosity of MgO nanofluid

When the nanoparticle volume concentration is lower than 5%, the viscosity of nanofluid can be obtained by using Drew and Passman viscosity correlation equation as shown in Eq. (4) [22].

$$\mu_{nf} = \mu_{bf}(1 + 2.5\emptyset) \quad (4)$$

Where: μ_{nf} is the viscosity of magnesium oxide nanofluid and μ_{bf} is the viscosity of base fluid.

Nanofluids show unique features regarding their thermal performances. The thermo-physical properties of nanofluid are different from the thermo-physical properties of conventional heat transfer fluids. The thermo-physical properties of MgO nanofluid is calculated based on Eq. (1) to Eq. (4) and the results are shown in Table 1.

Table 1
Thermo-physical properties of Magnesium Oxide nanofluid

Volume fraction (Ø), %	Density, $\boldsymbol{kg/m^3}$	Specific heat, $\boldsymbol{J/kg.k}$	Thermal conductivity, $\boldsymbol{W/m.k}$	Viscosity, $\boldsymbol{kg/m.s}$
0	1000	4180	0.6	1.003×10^{-3}
1	1025.8	4070	0.66498	1.1685×10^{-3}
2	1051.6	3965.527	0.681054	1.197×10^{-3}
3	1077.4	3865.994	0.6983107	1.2255×10^{-3}
4	1103.2	3771.117	0.71684	1.254×10^{-3}
5	1129	3680.576	0.7368408	1.2825×10^{-3}

3. Results

3.1 Validation of Results

A comparison between the results of this research and numerical results of research by Molana and Salem Banooni [24] are shown in Figure 4. The dimensionless analysis was carried out to compare the result of the numerical solution of this study with the result which was obtained by Molana and Salem Banooni [24]. The numerical solution showed a good agreement with Molana and Salem Banooni [24] result where the discretization errors are less than 10%.

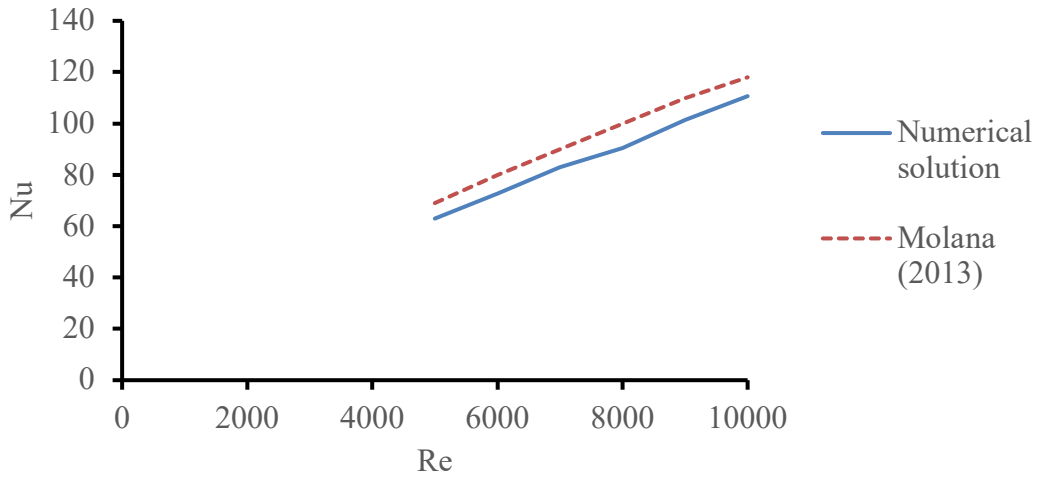

Fig. 4. Validation of result

3.2 Effect of Flow Distribution on the Heat Transfer Coefficient

The flow of jet impingement can be analysed from the vector diagram as shown in Figure 5. Based on the vector diagram obtained, there are several regions or phenomenon can be observed which is the stagnation region, stagnation point, fountain, jet core and jet deflection.

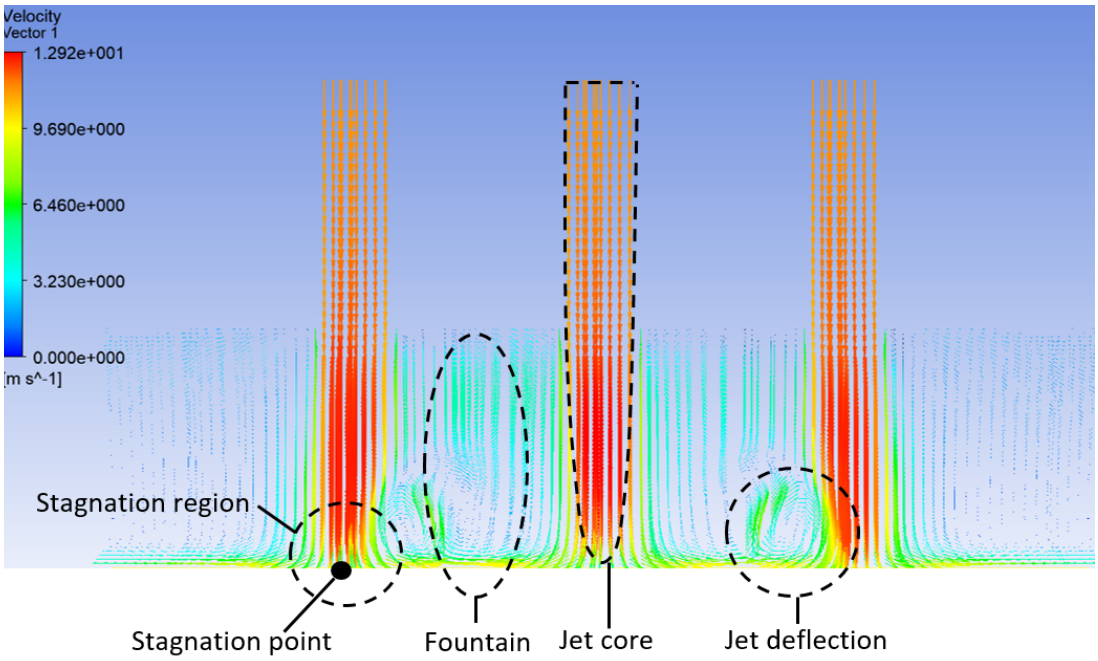

Fig. 5. Flow distribution of jet impingement

The spreading flow patterns are as shown in Table 2. As the Reynolds number increases, the velocity of flow increases. Higher heat transfer is observed at higher Re because of the increment of flow displacement at the impingement zone and the heat will de dissipated away faster by the MgO nanofluid.

Table 2
Contour of velocity distribution at various Re

Velocity distribution			
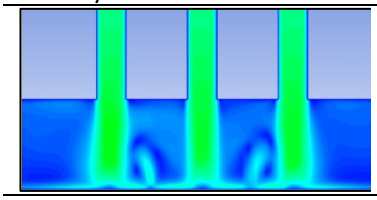	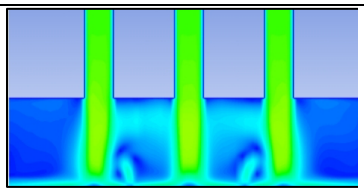	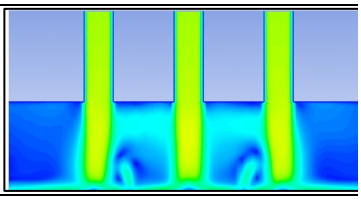	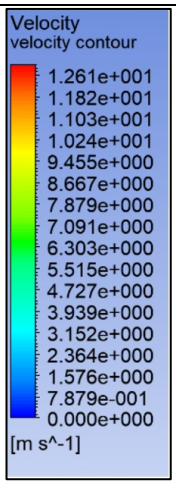
Re 5000	Re 6000	Re 7000	
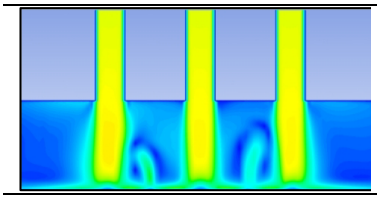	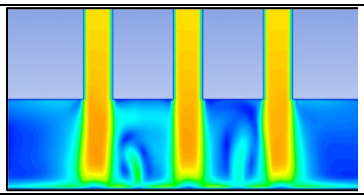	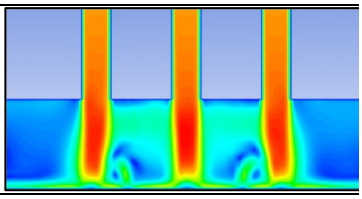	
Re 8000	Re 9000	Re 10000	

At the jet core, the centreline velocity of the impingement jet remains constant and same as the nozzle exit velocity. Stagnation point can be found at the surface of the target plate in the flow field of impingement jet. Based on Bernoulli's equation, the static pressure or stagnation pressure is highest as the velocity of the flow field is zero and thus the stagnation pressure is maximum at the stagnation point. It is observed that at the stagnation point, the heat transfer coefficient is the lowest. This is due to the flow velocity at stagnation point is zero and are forced to rest by the target plate. At the jet deflection zone, the velocity of the fluid flow is higher than the velocity at stagnation zone. Thus, resulting in higher heat transfer coefficient as compared to heat transfer coefficient at fountain and stagnation point. The fountain resulting from impact of flow on the plate and can be observed clearly between two adjacent jets. The deflection of flow from the two adjacent jets will interfere with each other and reduce the velocity at that region. This will cause the heat transfer coefficient to be lower.

As the region with higher flow velocity, the difference in temperature of the plate is higher. This is due to the region will be cooled faster. Since the heat transfer coefficient is dependent on the difference in temperature, as the larger the temperature difference, the greater the heat transfer coefficient. Thus, it can be said that higher velocity will results in higher heat transfer coefficient and vice versa.

3.3 Local Heat Transfer Distribution on Target Plate

Heat was transported from the heater to the target plate's bottom surface and dissipated by convection to the upper surface of the plate. It is observed that the regions of the target plate directly under the nozzle area were cooled slower than the other area. This is due to the stagnation region phenomenon whereby the fluid is trapped inside the region [25].

To determine the local heat transfer coefficient of het impingement, an evaluation line is constructed as shown in Figure 6. Based on the observation, as the Re increases, the wall adjacent temperature decreases and the heat transfer coefficient increases. Moreover, the heat transfer coefficient also increases as volume concentration increases.

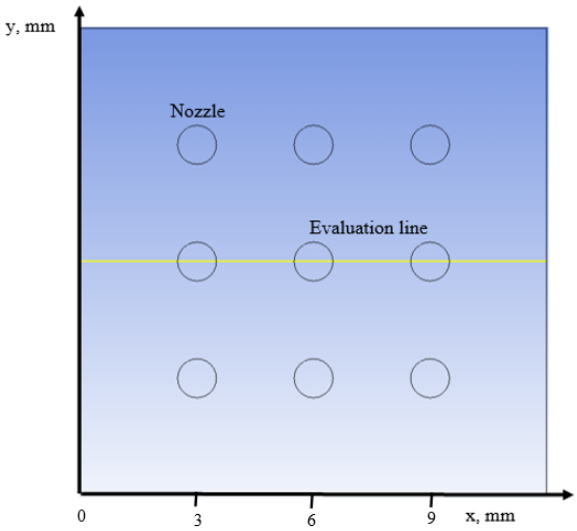

Fig. 6. Position of evaluation line of the local temperature

Table 3 represent the contour of heat transfer coefficient of target plate of impingement jet at Re=5000, 6000, 7000, 8000, 9000 and 10000 respectively for volume concentration 0%, 1%, 2%, 3%, 4% and 5%.

Table 3
Contour of heat transfer coefficient

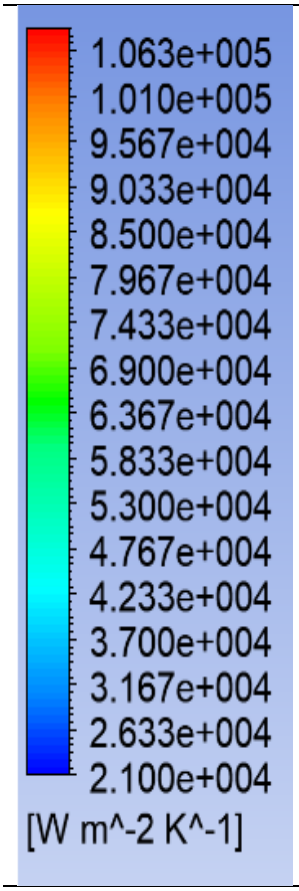

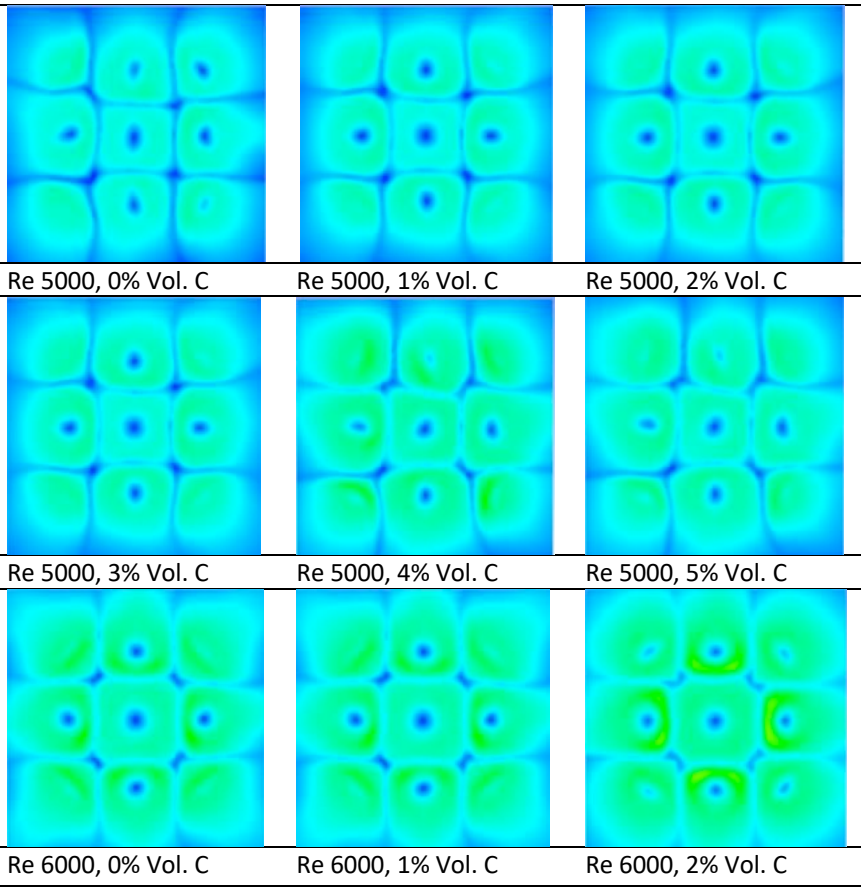

Re 5000, 0% Vol. C	Re 5000, 1% Vol. C	Re 5000, 2% Vol. C
Re 5000, 3% Vol. C	Re 5000, 4% Vol. C	Re 5000, 5% Vol. C
Re 6000, 0% Vol. C	Re 6000, 1% Vol. C	Re 6000, 2% Vol. C

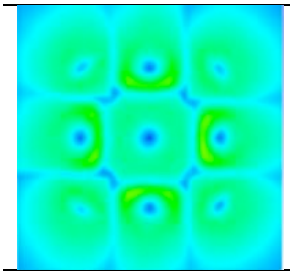	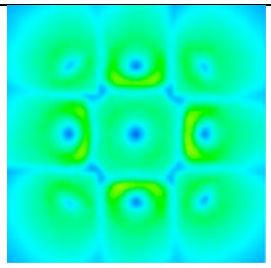	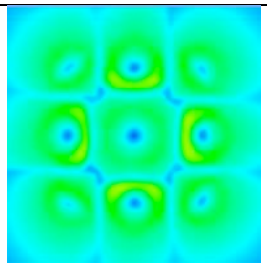	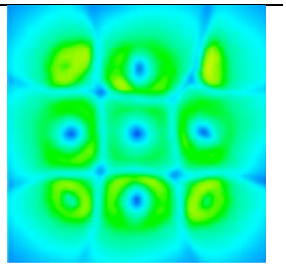
Re 6000, 3% Vol. C	Re 6000, 4% Vol. C	Re 6000, 5% Vol. C	Re 7000, 0% Vol. C
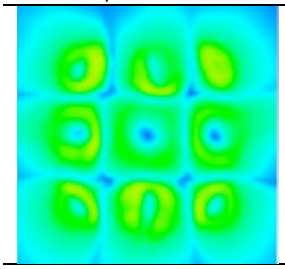	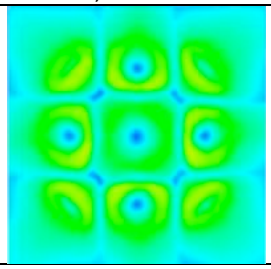	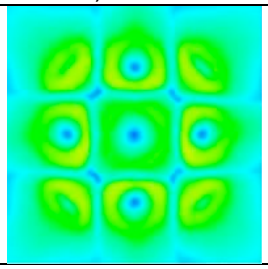	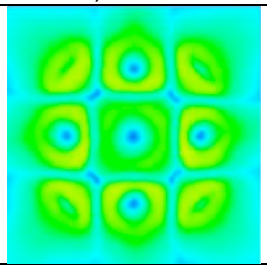
Re 7000, 1% Vol. C	Re 7000, 2% Vol. C	Re 7000, 3% Vol. C	Re 7000, 4% Vol. C
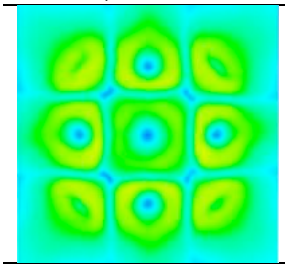	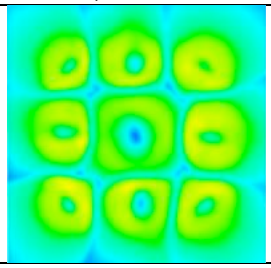	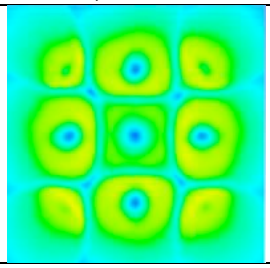	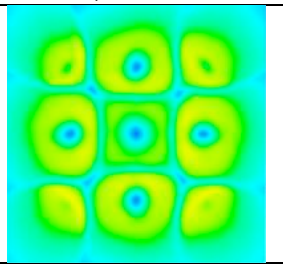
Re 7000, 5% Vol. C	Re 8000, 0% Vol. C	Re 8000, 1% Vol. C	Re 8000, 2% Vol. C
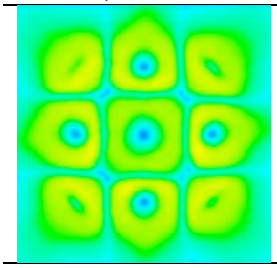	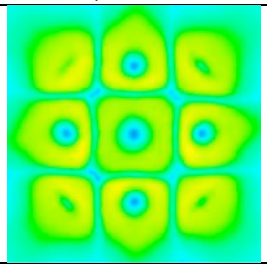	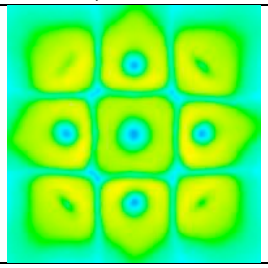	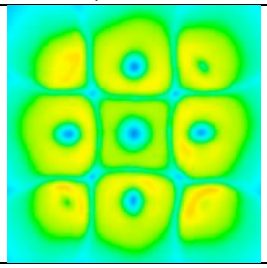
Re 8000, 3% Vol. C	Re 8000, 4% Vol. C	Re 8000, 5% Vol. C	Re 9000, 0% Vol. C
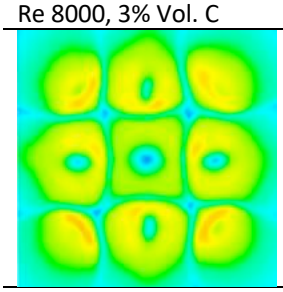	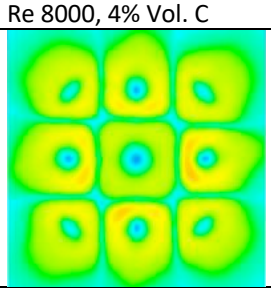	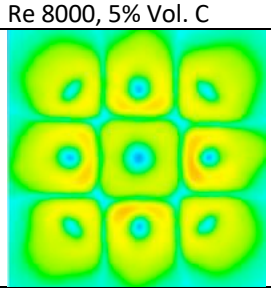	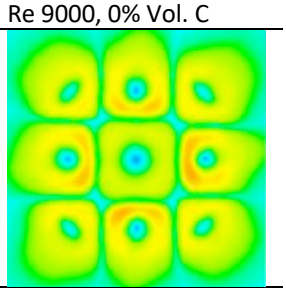
Re 9000, 1% Vol. C	Re 9000, 2% Vol. C	Re 9000, 3% Vol. C	Re 9000, 4% Vol. C
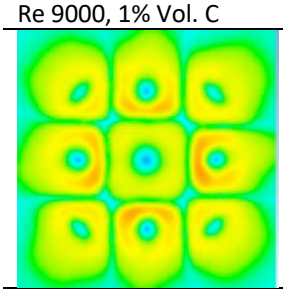	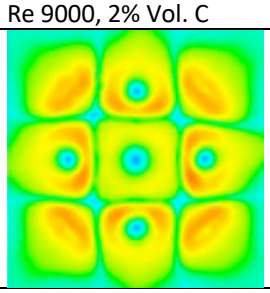	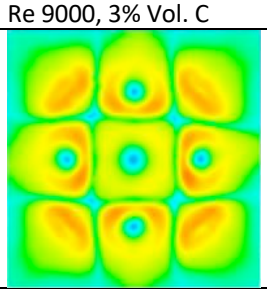	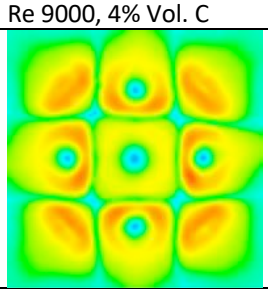
Re 9000, 5% Vol. C	Re 10000, 0% Vol. C	Re 10000, 1% Vol. C	Re 10000, 2% Vol. C

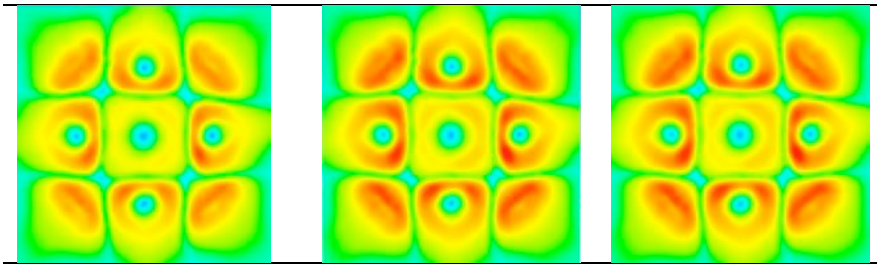

Re 10000, 3% Vol. C	Re 10000, 4% Vol. C	Re 10000, 5% Vol. C

For local wall heat transfer coefficient along the evaluation line, it is observed that when the heat transfer coefficient increases as the Re increases. Enhancement of local heat transfer coefficient can be also done by increase the volume concentration of MgO nanofluid. Figure 7 represent the local wall heat transfer coefficient along the evaluation line for various Re at 5% volume concentration.

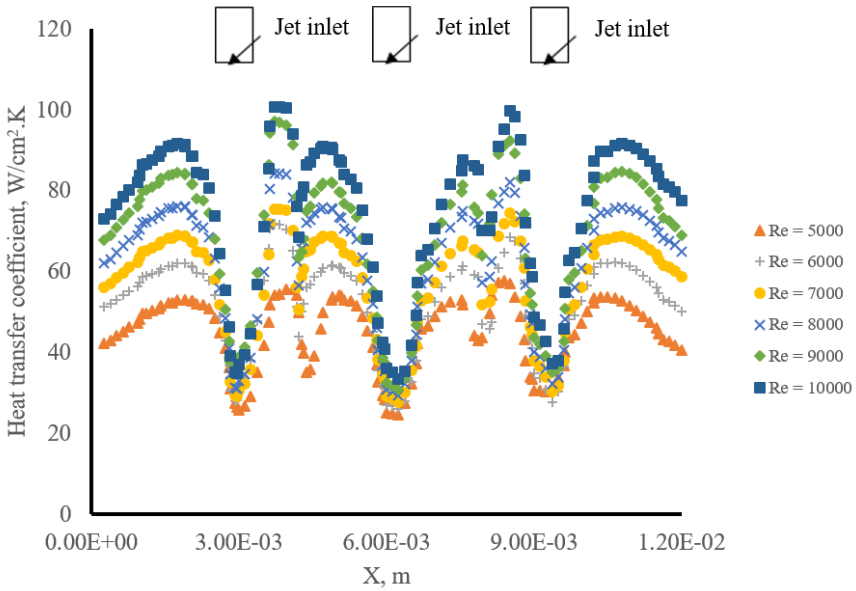

Fig. 7. Local surface heat transfer coefficient for various Re at 5% volume concentration

While Figure 8 represent the local wall heat transfer coefficient distribution along the evaluation line for various volume concentration at Re 5000. Based on the observation, the target plate has the lowest heat transfer coefficient at the stagnation point (X=3, 6 and 9 mm). This phenomenon is due to the flow field velocity equals to zero at the stagnation point whereby the flow velocity are forced to rest when it collides with the target plate. The region around the stagnation point showed higher local heat transfer coefficient than that of stagnation point. This is due to at the jet deflection zone, the velocity of jet is higher than the velocity of flow at stagnation point. At the 'fountain', the heat transfer coefficient decreases slightly as compared to the jet deflection zone. This is due to the interference of flow of two adjacent jet. The velocity of flow decreases at the region and thus reduce the heat transfer coefficient.

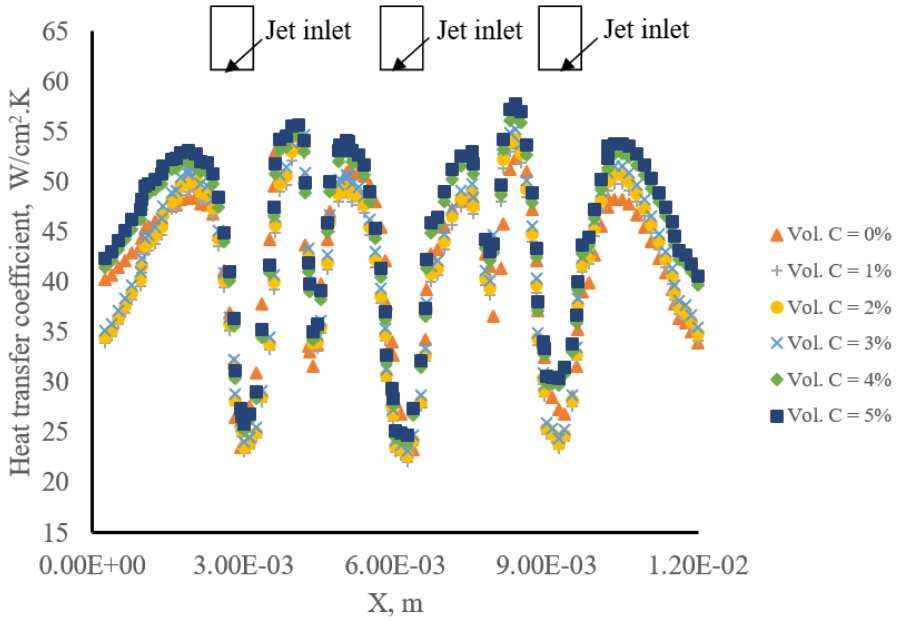

Fig. 8. Local surface heat transfer coefficient for various volume concentration at Re 5000

3.4 Effect of Volume Concentration on Heat Transfer Coefficient

The results in Figure 9 show the influence of volume concentration on the heat transfer coefficient. The overall heat transfer coefficient of water as Re increases. It was observed that as the Re and volume concentration of MgO nanofluid increases, the surface average heat transfer coefficient increases. The maximum value of surface average heat transfer coefficient of 79.6311 W/cm2.K is observed at the maximum Re and 5% volume concentration while the lowest surface average heat transfer coefficient of 41.4598 W/cm2.K was observed at the minimum Re and 0% volume concentration. Yazdi *et al.,* [26] noted a significant enhancement in heat transfer when MgO nanofluid concentration was increased beyond 3%, indicating the potential for optimized nanofluid mixtures. Hanafi *et al.,* [27] also demonstrated that nanofluids with higher concentrations of nanoparticles lead to enhanced convective heat transfer in impingement jet systems.

The increasing trend of the heat transfer coefficient of nanofluid is because of the nanoparticles which existing in the base fluid enhance the viscosity and thermal conductivity of the base fluid. The enhancement of the viscosity and thermal conductivity of nanofluid leads to the enhancement of heat transfer coefficient [26].

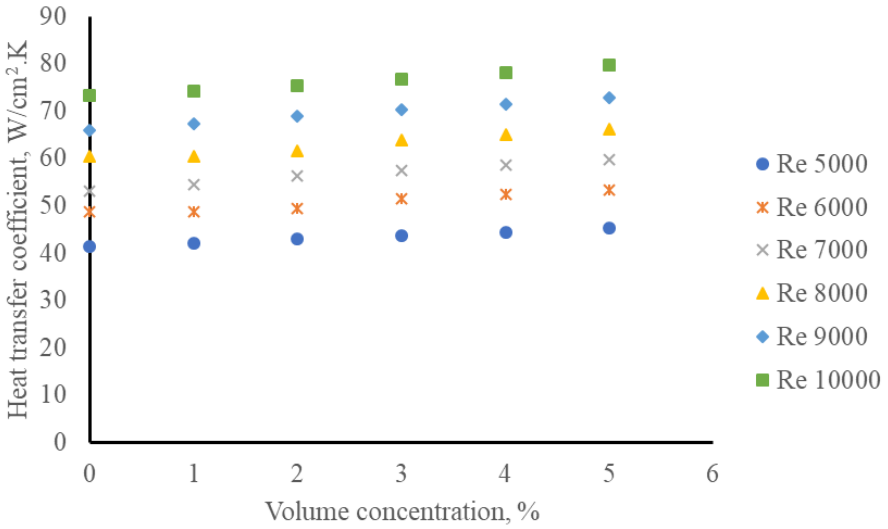

Fig. 9. Influence of volume concentration on heat transfer coefficient of MgO nanofluids at different Re

3.5 Effect of Reynolds Number on Heat Transfer Coefficient

The results in Figure 10 indicates the effect of Re on the heat transfer coefficient. It was observed that when Re increases, the heat transfer coefficient increases while the thermal resistance decreases. The increasing trend is expected and well agreed with the fundamental principles of convective flow. This is because by increasing the Reynolds number, the thermal boundary layers thickness decreases and thus results in the increasing heat transfer coefficient . Moreover, the mass flow rate will increase as Reynolds number of flow increase, thus amplified the forced convection heat transfer coefficient on the target plate. Based on the result obtained, the maximum heat transfer coefficient was obtained at Reynolds number 10000 and 5% volume concentration where the value of 79.6311 W/cm2.K was observed. Balla *et al.,* [28] research noted a linear relationship between increasing Reynolds numbers and the improvement of heat transfer rates in impingement jet systems.

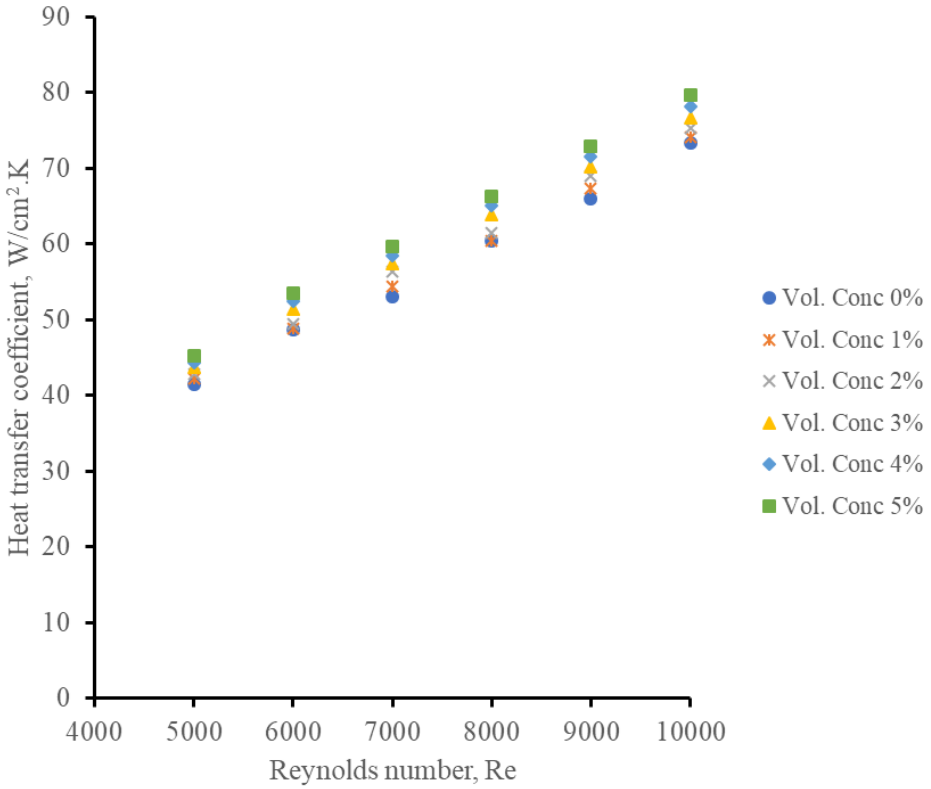

Fig. 10. Influence of Re on heat transfer coefficient of MgO nanofluids at different volume concentration

3.6 Heat Transfer Coefficient of Various Nanofluid

The thermo-physical properties of the nanofluids were determined by the Eq. (1) to Eq. (4) mentioned in the previous section and as shown in Table 4. Results of Reynolds number 10000, 5% volume concentration of MgO nanofluid was compared with TiO2, Al2O3 and SiO2 nanofluid with same Re and volume concentration.

Table 4
Thermo-physical properties of various nanofluids

	TiO_2	Al_2O_3	SiO_2	MgO
Re 10000, 5% Vol. Concentration				
Density	1152.5	1149	1082.5	1129
Specific heat	3568.0195	3621.449	3757.7136	3680.576
Heat conductivity	0.7227	0.73469	0.6658	0.7368408
Viscosity	1.2825e-3	1.2825e-3	1.2825e-3	1.2825e-3
Velocity	11.12798	11.1619	11.84	11.35961

Figure 11 represent the local heat transfer coefficient distribution along the centreline of various nanofluids. Based on the result along the centreline, it can be observed that MgO nanofluid have the highest heat transfer coefficient followed by Al2O3 nanofluid, TiO2 nanofluid and SiO2 nanofluid. It was observed that as the thermal conductivity of the nanofluids increase, the heat transfer coefficient of the impingement jet increases, research by Hanafi *et al.,* [29] also supports this finding. Etminan and Harun [30] has also demonstrated that increasing nanoparticle volume concentration leads to an enhancement in the overall thermal conductivity of the nanofluid. In addition, Verma *et*

al., [31] compared various working fluids and found that MgO nanofluids outperformed other fluids like CuO and MWCNTs in terms of heat transfer efficiency.

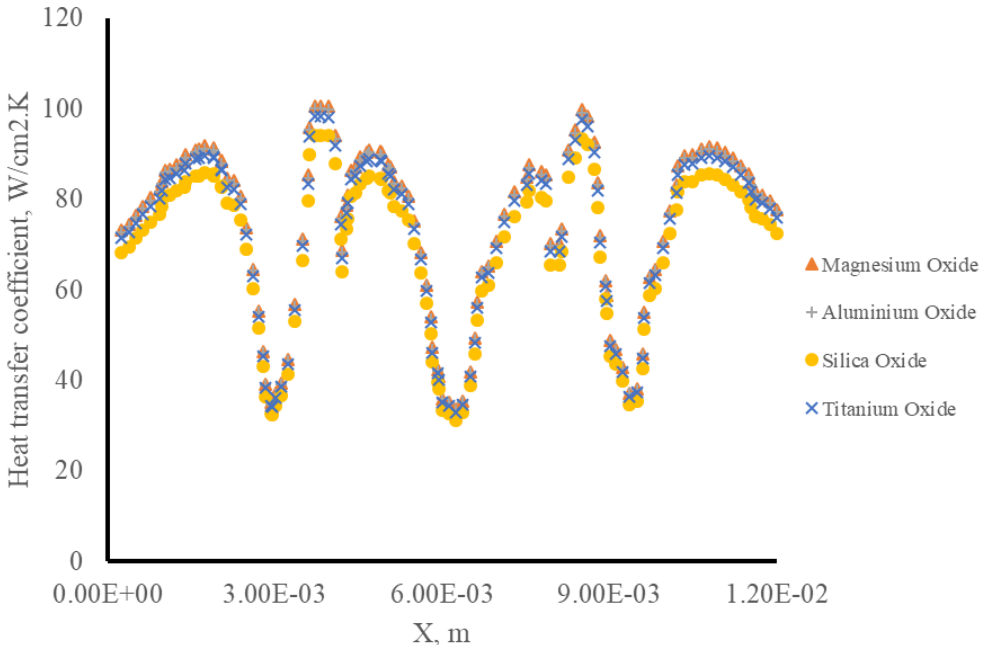

Fig. 11. Local heat transfer coefficient distribution along the evaluation line for various nanofluids at Re=10000 and volume concentration = 5%

4. Conclusion

Based on the numerical simulation that had been conducted, the following conclusion can conclude that:

i. The flow region of the impingement jet can be observed at the vector plot of the result.
ii. The heat transfer coefficient of impingement jet was greater than that of traditional heat transfer fluid such as water in this case.
iii. The heat transfer coefficient can be enhanced by increasing the Reynolds number and volume concentration of the nanofluid flow.
iv. The heat transfer coefficient can be enhanced by increasing the thermal conductivity of nanofluid. Based on the results of comparing various nanofluids, the nanofluid with greater thermal conductivity have larger heat transfer coefficient value. While the nanofluid with lowest thermal conductivity shows lowest heat transfer coefficient.

Acknowledgement
The research has been funded by the Ministry of Higher Education (MOHE) Malaysia, Malaysia under the Fundamental Research Grant Scheme with grant number FRGS/1/2021/TK0/UKM/03/2 and FRGS/1/2015/TK07/UTHM/02/4. It is also funded by Universiti Kebangsaan Malaysia (UKM), Malaysia under TP-K017153.

References

[1] Liu, X. and J. H. Lienhard. "Extremely high heat fluxes beneath impinging liquid jets." *ASME Journal of Heat Transfer* 115, no. 2 (1993): 472-476. https://doi.org/10.1115/1.2910703

[2] Ewe, Win Eng, Ahmad Fudholi, Kamaruzzaman Sopian, Evgeny Solomin, Mohammad Hossein Yazdi, Nilofar Asim, Noshin Fatima *et al.,* "Jet impingement cooling applications in solar energy technologies: Systematic literature review." *Thermal Science and Engineering Progress* 34 (2022): 101445. https://doi.org/10.1016/j.tsep.2022.101445

[3] Tang, Tsz Loong, Hamidon Salleh, Muhammad Imran Sadiq, Mohd Anas Mohd Sabri, Meor Iqram Meor Ahmad and Wan Aizon W. Ghopa. "Experimental and Numerical Investigation of Flow Structure and Heat Transfer Behavior of Multiple Jet Impingement Using MgO-Water Nanofluids." *Materials* 16, no. 11 (2023): 3942. https://doi.org/10.3390/ma16113942

[4] Hasan, Husam Abdulrasool, Kamaruzzaman Sopian and Kayser Aziz Ameen. "Numerical investigation of Microjet impingement of water for cooling photovoltaic solar cell." *Journal of Advanced Research in Fluid Mechanics and Thermal Sciences* 51, no. 1 (2018): 71-79.

[5] Salleh, Hamidon, Amir Khalid, Syabillah Sulaiman, Bukhari Manshoor, Izzuddin Zaman, Shahrin Hisham Amirnordin, Amirul Asyraf and Wahid Razzaly. "Effects of fluid flow characteristics and heat transfer of integrated impingement cooling structure for micro gas turbine." *CFD Letters* 12, no. 9 (2020): 104-115. https://doi.org/10.37934/cfdl.12.9.104115

[6] Waware, N. S. Y., N. S. S. Kore and N. S. P. Patil. "Heat Transfer Enhancement in Tubular Heat Exchanger with Jet Impingement: A Review." Journal of Advanced Research in Fluid Mechanics and Thermal Sciences 101, no. 2 (2023): 8–25. https://doi.org/10.37934/arfmts.101.2.825.

[7] Zhou, Mingzheng, Guodong Xia and Lei Chai. "Heat transfer performance of submerged impinging jet using silver nanofluids." *Heat and Mass Transfer* 51 (2015): 221-229. https://doi.org/10.1007/s00231-014-1387-0

[8] Bergles, Arthur E. *High-flux processes through enhanced heat transfer*. 2003.

[9] Zuckerman, N. and Noam Lior. "Jet impingement heat transfer: physics, correlations and numerical modeling." *Advances in heat transfer* 39 (2006): 565-631. https://doi.org/10.1016/S0065-2717(06)39006-5

[10] Tomac, Maximilian and David Eller. "From geometry to CFD grids—an automated approach for conceptual design." *Progress in Aerospace Sciences* 47, no. 8 (2011): 589-596. https://doi.org/10.1016/j.paerosci.2011.08.005

[11] ANSYS Inc. "ANSYS Fluent 18.1 Theory Guide." *ANSYS Inc.*

[12] Chougule, N. K., G. V. Parishwad, P. R. Gore, S. Pagnis and S. N. Sapali. "CFD analysis of multi-jet air impingement on flat plate." In *Proceedings of the world congress on Engineering*, vol. 3, pp. 2078-0958. 2011.

[13] Faris Abdullah, Mahir, Rozli Zulkifli, Zambri Harun, Shahrir Abdullah and Wan Aizon Wan Ghopa. "Experimental and numerical simulation of the heat transfer enhancement on the twin impingement jet mechanism." *Energies* 11, no. 4 (2018): 927. https://doi.org/10.3390/en11040927

[14] Jehad, D. G., G. A. Hashim, A. Kadhim Zarzoor and CS Nor Azwadi. "Numerical study of turbulent flow over backward-facing step with different turbulence models." *Journal of Advanced Research Design* 4, no. 1 (2015): 20-27.

[15] Karimi, Mohsen, Guven Akdogan and Steven M. Bradshaw. "EFFECTS OF DIFFERENT MESH SCHEMES AND TURBULENCE MODELS IN CFD MODELLING OF STIRRED TANKS." *Physicochemical Problems of Mineral Processing* 48, no. 2 (2012).

[16] Kulkarni, Siddharth Suhas, Craig Chapman and Hanifa Shah. "Computational fluid dynamics (CFD) mesh independency study of A straight blade horizontal Axis tidal turbine." (2016). https://doi.org/10.20944/preprints201608.0008.v1

[17] Putranto, Vicky Adrian and Allessandro Utomo. "Interaction Analysis of Micro Bubbles in the Flat Plate to Reduce Drag using Computational Fluid Dynamic." *Semarak Engineering Journal* 4, no. 1 (2024): 18-28.

[18] Nasir, Muhammad Nabihan Arif, Nolia Harudin, Farah Elida Selamat and Zulkifli Marlah. "Development Of Enhanced Taguchi's T-Method Model in Predicting Energy Demand." *Semarak Engineering Journal* 1, no. 1 (2023): 34-45.

[19] Ng, Fei Chong, Aizat Abas, Muhammad Hafifi Hafiz Ishak, Mohd Zulkifly Abdullah and Abdul Aziz. "Effect of thermocapillary action in the underfill encapsulation of multi-stack ball grid array." *Microelectronics Reliability* 66 (2016): 143-160. https://doi.org/10.1016/j.microrel.2016.10.001

[20] Abdul-Rahman, H., H. Moria and Mohammad Rasidi Mohammad Rasani. "Aerodynamic study of three cars in tandem using computational fluid dynamics." *Journal of Mechanical Engineering and Sciences* 15, no. 3 (2021): 8228-8240. https://doi.org/10.15282/15.3.2021.02.0646

[21] Zainodin, Syafiq, Anuar Jamaludin, Roslinda Nazar and Ioan Pop. "Impact of heat source on mixed convection hybrid ferrofluid flow across a shrinking inclined plate subject to convective boundary conditions." *Alexandria Engineering Journal* 87 (2024): 662-681. https://doi.org/10.1016/j.aej.2023.12.057

[22] Wang, Xiang-Qi and Arun S. Mujumdar. "Heat transfer characteristics of nanofluids: a review." *International journal of thermal sciences* 46, no. 1 (2007): 1-19. https://doi.org/10.1016/j.ijthermalsci.2006.06.010

[23] Safiei, Wahaizad, Md Mustafizur Rahman, Ratnakar Kulkarni, Md Noor Ariffin and Zetty Akhtar Abd Malek. "Thermal conductivity and dynamic viscosity of nanofluids: a review." *Journal of Advanced Research in Fluid Mechanics and Thermal Sciences* 74, no. 2 (2020): 66-84. https://doi.org/10.37934/arfmts.74.2.6684

[24] Molana, M. and Salem Banooni. "Investigation of heat transfer processes involved liquid impingement jets: a review." *Brazilian Journal of Chemical Engineering* 30 (2013): 413-435. https://doi.org/10.1590/S0104-66322013000300001

[25] Jambunathan, K., Eliza Lai, MAm Moss and B. L. Button. "A review of heat transfer data for single circular jet impingement." *International journal of heat and fluid flow* 13, no. 2 (1992): 106-115. https://doi.org/10.1016/0142-727X(92)90017-4

[26] Yazdi, Mohammad H., Evgeny Solomin, Ahmad Fudholi, Ghasem Divandari, Kamaruzzaman Sopian and Perk Lin Chong. "Thermal performance of nanofluid flow inside evacuated tube solar collector." *International Journal of Heat and Technology* 39, no. 4 (2021): 1262-1270. https://doi.org/10.18280/ijht.390424

[27] Hanafi, Nur Syahirah M., Wan Aizon W. Ghopa, Rozli Zulkifli, Mohd Anas Mohd Sabri, Wan Fathul Hakim W. Zamri and Meor Iqram Meor Ahmad. "Mathematical formulation of Al2O3-Cu/water hybrid nanofluid performance in jet impingement cooling." *Energy Reports* 9 (2023): 435-446. https://doi.org/10.1016/j.egyr.2023.06.035

[28] Balla, Hyder H., Shahrir Abdullah, Emad A. Jaffar Al-Mulla, Wan Mohd Faizal Wan Mahmood, Rozli Zulkifli and Kamaruzaman Sopian. "Effect of Reynolds number on heat transfer and flow for multi-oxide nanofluids using numerical simulation." *Research on Chemical Intermediates* 39 (2013): 2197-2210. https://doi.org/10.1007/s11164-012-0750-3

[29] Hanafi, Nur Syahirah M., Wan Aizon W. Ghopa, Rozli Zulkifli, Shahrir Abdullah, Zambri Harun and Mohd Radzi Abu Mansor. "Numerical simulation on the effectiveness of hybrid nanofluid in jet impingement cooling application." *Energy Reports* 8 (2022): 764-775. https://doi.org/10.1016/j.egyr.2022.07.096

[30] Etminan, A. and Z. Harun. "Forced convective heat transfer analysis for two-dimensional slot jet of water-CuO Nanofluid." *J. Kejuruteraan* 33 (2021): 229-238. https://doi.org/10.17576/jkukm-2021-33(2)-08

[31] Verma, Sujit Kumar, Arun Kumar Tiwari, Sandeep Tiwari and Durg Singh Chauhan. "Performance analysis of hybrid nanofluids in flat plate solar collector as an advanced working fluid." *Solar Energy* 167 (2018): 231-241. https://doi.org/10.1016/j.solener.2018.04.017